Journal of
Medicinal Chemistry

Article

Synthesis and in vitro and in vivo biological evaluation of tissue-specific bisthiazole Histone deacetylase (HDAC) inhibitors

Shu-Wei Zhang, Chao-Jun Gong, Ming-Bo Su, Fei Chen, Ting He, Yang-Ming Zhang, Qian-Qian Shen, Yi Su, Jian Ding, Jia Li, Yi Chen, and Fa-Jun Nan

J. Med. Chem., **Just Accepted Manuscript** • DOI: 10.1021/acs.jmedchem.9b01792 • Publication Date (Web): 19 Dec 2019

Just Accepted

is published by the American Chemical Society. 1155 Sixteenth Street N.W., Washington, DC 20036

Synthesis and in vitro and in vivo biological evaluation of tissue-specific bisthiazole histone deacetylase (HDAC) inhibitors

*Shu-Wei Zhang,†,§,‖ Chao-Jun Gong,†,‖ Ming-Bo Su,† Fei Chen,† Ting He,† Yang-Ming Zhang,†,# Qian-Qian Shen,‡ Yi Su‡ Jian Ding,‡ Jia Li,† * Yi Chen, ‡* Fa-Jun Nan†,#**

† State Key Laboratory of Drug Research, the National Center for Drug Screening, Shanghai Institute of Materia Medica, Chinese Academy of Sciences, Shanghai, 201203, China;

Yantai Key Laboratory of Nanomedicine & Advanced Preparations, Yantai Institute of Materia Medica, Shandong, 264000, China；

‡ Division of Antitumor Pharmacology, State Key Laboratory of Drug Research, Shanghai Institute of Materia Medica, Chinese Academy of Sciences, Shanghai 201203, China

§ University of Chinese Academy of Sciences, No.19A Yuquan Road, Beijing, 100049, P. R. China

‖ These authors contributed equally

KEYWORDS*: Histone deacetylase inhibitors; Bisthiazole; Solid tumor.*

ABSTRACT: A series of bisthiazole-based hydroxamic acids as novel potent HDAC inhibitors was developed during our previous work. In the present work, a new series of highly potent bisthiazole-based compounds were designed and synthesized. Among the prepared compounds, compound **H13**, which contains an α-(S)-methyl-substituted benzyl group, displays potent inhibitory activity towards human HDACs and several cancer cells lines. Compound **H13** has a favorable PK profile and high tissue distribution specificity in the colon, as well as good efficacy in the AOM-DSS mouse model for colitis-associated colonic tumorigenesis.

Introduction

The acetylation and deacetylation of histones play a key role in the structural modification of nuclear chromatin and are regulated by the activity of histone acetyltransferase (HAT) and histone deacetylase (HDAC), respectively.[1] Abnormal expression of HDACs has been associated with various types of cancers. HDAC inhibitors (HDACi) can inhibit the activity of HDAC and display obvious antitumor activity by changing the histone acetylation state, causing tumor cell growth arrest and inducing differentiation and apoptosis. Thus, HDAC inhibitors are widely used in cancer therapy.[2] To date, five HDAC inhibitors have been approved by the FDA (**Figure 1**). SAHA[3], FK-228 (romidepsin)[4], belinostat[5], and chidamide[6] are used for treating cutaneous T-cell lymphoma (CTCL) or peripheral T-cell lymphoma (PTCL), and LBH589 (panobinostat)[7] is the first HDAC inhibitor approved for multiple myeloma (MM).

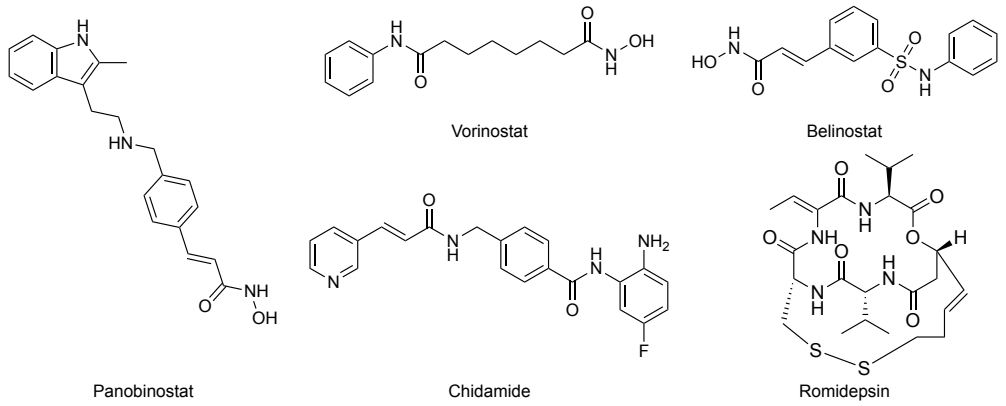

Figure 1. Approved HDAC Inhibitors

It is well known that most HDAC inhibitors are highly effective in hematological malignancy. However, in solid tumors, the results are not as promised. For example, many clinical trials of SAHA and FK-228 on breast, colorectal, and prostate cancers and other solid tumors have been conducted. Unfortunately, the results were not ideal, and various side effects such as prolonged QT intervals, anorexia, weakness, diarrhea, fatigue, vomiting, anemia, and leukocyte reduction were reported.[8] Therefore, the development of new HDAC inhibitors for solid tumor therapy is an ongoing challenge.

In our previous work, we identified a series of bisthiazole-based HDAC inhibitors that were inspired by the natural potent HDAC inhibitor largazole. Of those compounds, the simple but potent compound **H1 (Bisthianostat)**[9,10] was selected as a candidate for further development for multiple myeloma(NCT03618602). In this paper, we report further structural modifications of these bisthiazole HDAC inhibitors through changes to the linker group between the hydroxamate and the bisthiazole core (**Figure 2**) and through varying the substituents on the core structure. Thus, we demonstrated that compounds with an α-(S)-methyl-substituted benzyl group as the linker had excellent potency in vitro and in vivo.

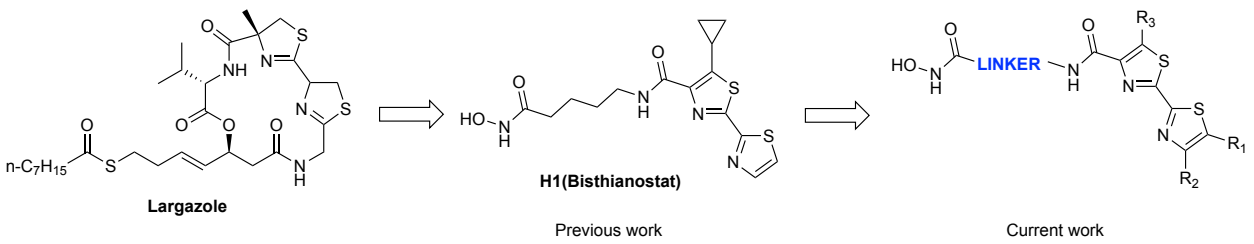

Figure 2. From Largazole to Bisthiazole HDAC Inhibitors

Chemistry

First, we kept the bisthiazole core structure and hydroxamates unchanged, but we replaced the aliphatic linker with heteroalkyl, benzyl or substituted benzyl groups. The syntheses of compounds **H2-H8** are outlined in Scheme 1. Acids **1a**[9] and **1b**[9] were condensed with different amines to afford amides **7-13**; treating these amides with hydroxylamine hydrochloride afforded compounds **H2-8** respectively.

Commercially available intermediates **14** and **15** were condensed to afford imine **16**.[13] Imine **16** was treated with different Grignard reagents to generate sulfinamides **17a-c**.[14] The diastereoisomers **17a** and **17b** could be isolated by silica gel chromatography. Deprotection of **17a-c** afforded chiral amines **18a-c**. Amines **18a-c** were condensed with various acids to afford amides **19a-c**. The amides were then converted to compounds **H6a-b** and **H9** through a similar route to what is shown in **Scheme 1.** To investigate the SAR in detail, the (S)-methyl benzyl linker was maintained, and a series of analogues with different substituents on the left-hand thiazole ring was designed and synthesized as outlined in **Scheme 3**. Various bisthiazole acids with substituents on the left-hand thiazole ring were coupled with chiral amine **18a** to give amides **21a-f**, which were converted to the final hydroxamates **H10-15** through a route similar to what is shown in **Scheme 2**.

Scheme 1. Synthesis of Compounds **H2-8.**

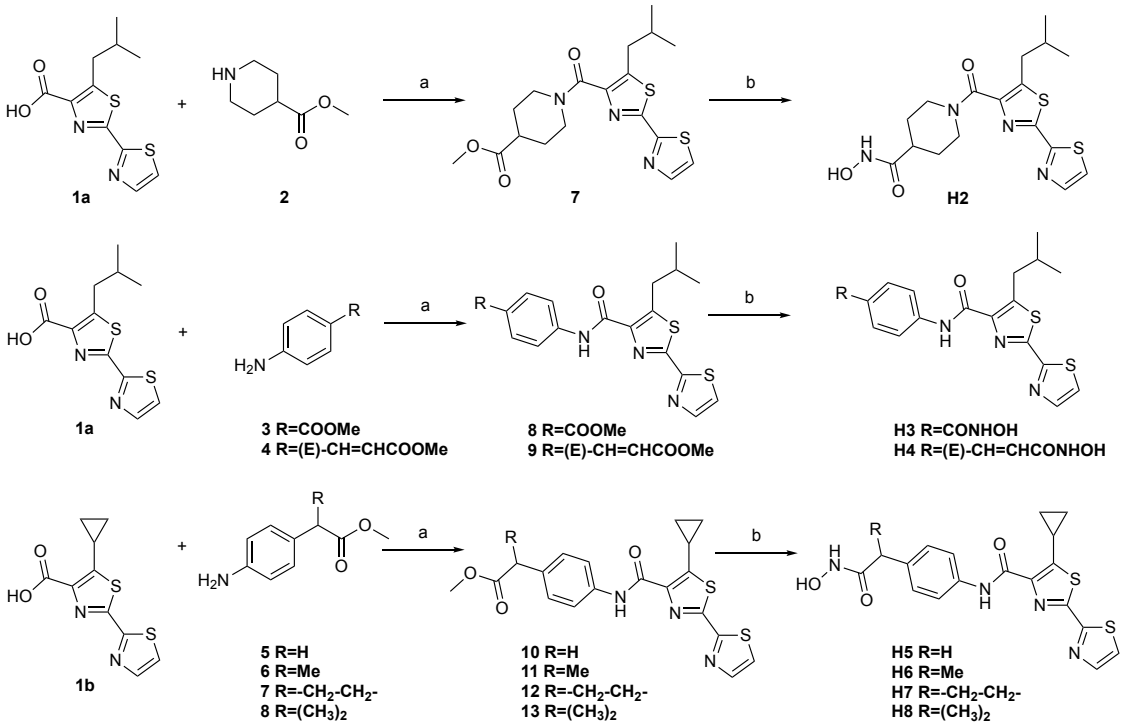

[a]Reagents and conditions: (a) EDCI, HOBt, i-Pr_2NEt, DMF, room temperature, 12h. (b) $NH_2OH{\cdot}HCl$, DBU, DCM:MeOH=1:1, room temperature, 12h.

Scheme 2. Synthesis of Compounds **H6a**, **H6b** and **H9.**

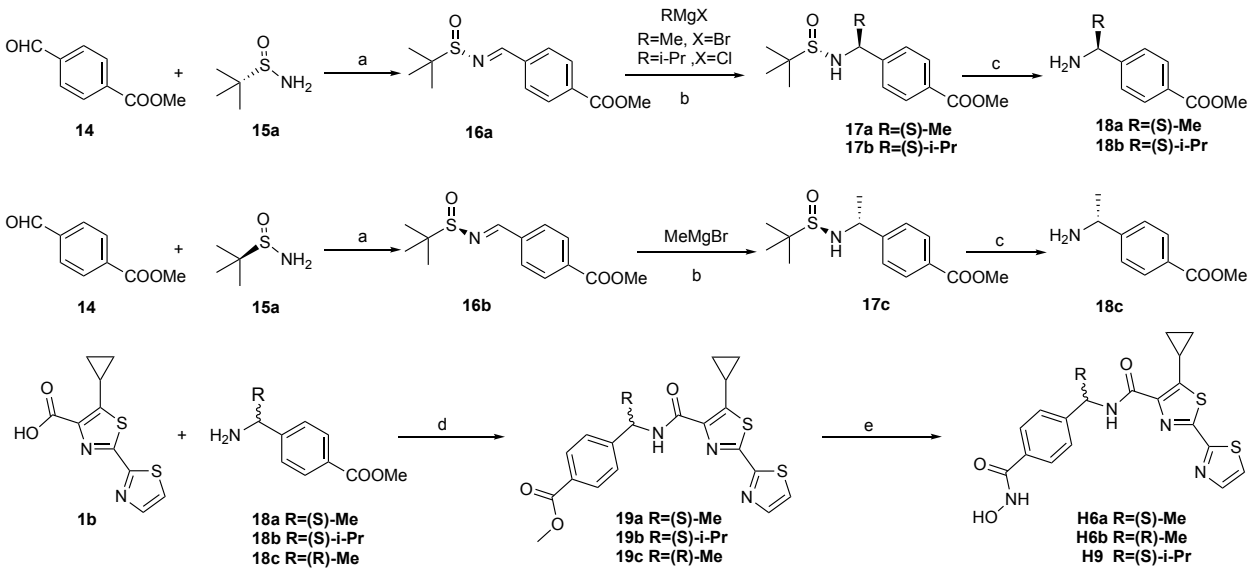

[a]Reagents and conditions: (a) Cs_2CO_3, DCM, reflux, 18 h. (b) Et_2Zn, THF, -78 °C, 4 h. (c) 2 N HCl/MeOH, DCM, room temperature, 3 h. (d) EDCI, DMAP, DCM, room temperature, 12 h. (e) $NH_2OH{\cdot}HCl$, DBU, DCM:MeOH=1:1, room temperature, 12 h.

Scheme 3. Synthesis of Compounds **H10-H15**.

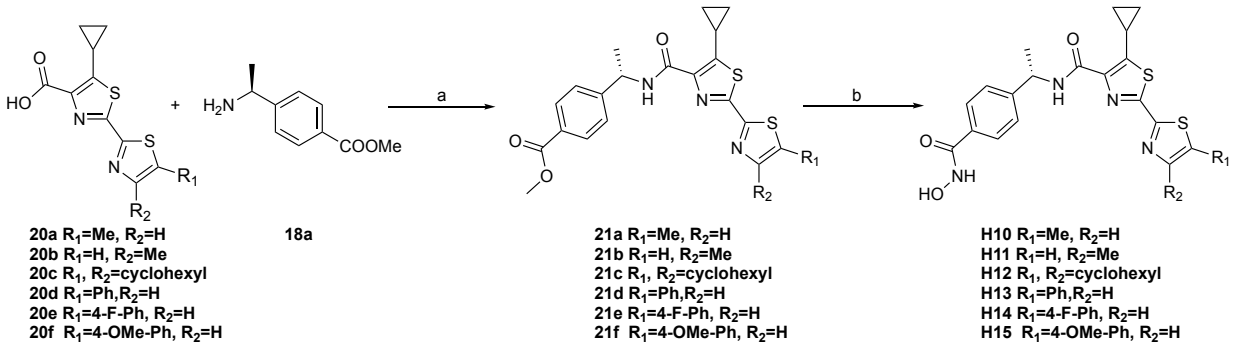

[a]Reagents and conditions: (a) EDCI, DMAP, DCM, room temperature, 12 h. (b) $NH_2OH{\cdot}HCl$, DBU, DCM:MeOH=1:1, room temperature, 12 h.

Results and discussion

HDAC Inhibition Assay

The inhibitory activities against human HDACs of compounds **H1-8** are shown in Table 1. Using LBH589 (panobinostat) as the control compound, compared to **H1**, changing the aliphatic linker to a heteroalkyl group (compound **H2**, **Table 1**) or a phenyl group decreased the inhibitory activity of the compound, and they were much less potent toward the HDACs (compounds **H3** and **H4**, **Table 1**). However, the compounds with a benzyl linker showed higher HDAC inhibitory activities (compounds **H5-8**), and compound **H5**, which has no substituents at the benzyl position, was more potent against human HDACs 1, 3, and 6 than **H1** with IC50 values of 30-40 nM (**Table 1**). Small α-substituents on the benzyl group were tolerated (compounds **H6-8**, **Table 1**).

Table 1. Inhibitory activity against human HDACs

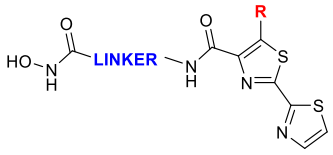

Compound	R	LINKER	IC_{50}(nM)		
			HDAC1	HDAC3	HDAC6
H1		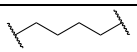	81.46±4.91	73.91±3.83	61.49±4.64
H2		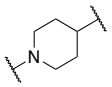	NA[a]	NA	NA
H3		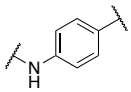	1020±200	690±90	300±50
H4		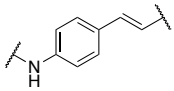	660±90	410±60	310±60
H5		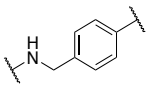	23.74±0.98	27.51±0.16	21.91±2.80
H6		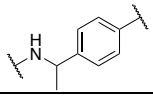	80.98±15.0	189±17	41.65±16.1

H7	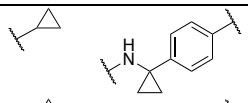	22.33±2.97	16.29±2.18	16.58±1.69
H8	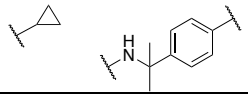	163.4±8	148±10	148±14
LBH589		7.03±1.18	5.83±1.09	10.63±1.30

NA[a] = No inhibitory activity observed at 20 μg/mL.

Considering the benzyl position is easily metabolized position in vivo, a substituent at the benzyl position was introduced to increase the metabolic stability in the same series. Further explorations focused on analogues with different configurations of α-substituted benzyl groups (**Table 2**), and the chirality of the α-methyl position of the benzyl group was crucial to the inhibitory activity. (S)-Methyl-substituted compound **H6a** was much more potent than its enantiomer **H6b** (IC_{50} values of 0.04 μM and 0.28 μM, respectively, against HDAC 1, **Table 2**). When the (S)-methyl group was exchanged for a bulkier (S)-isopropyl group, the inhibitory activity of the compound was the same as that of compound **H6a** (compound **H9**, **Table 2**). Preliminary docking study of **H6a** and **H6b** showed the chiral methyl group determines the orientation of the compound in the pocket, S-enantiomer preferentially makes the hydroxamic acid coordinates to zinc ions in the pocket than R-enantiomer. Therefore, it is reasonable to take **H6a** as a new starting point for further exploration (Information on computational modeling/docking studies is shown in Figure I, SI file).

Table 2. Inhibitory activity against human HDACs

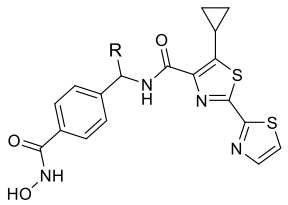

Compound	R	IC_{50}(nM)		
		HDAC1	HDAC3	HDAC6
H6	Me	80.98±15.0	189.4±16.7	41.65±16.1
H6a	(S)-Me	40.92±0.41	42.51±3.04	14.02±1.74

H6b	(R)-Me	279±5	260±22	211±36
H9	(S)-i-Pr	38.25±7.29	38.41±7.13	14.15±2.03
LBH589		7.03±1.18	5.83±1.09	10.63±1.30

Due to the importance of the (S)-methyl group on the benzyl linker, we then investigated a series of compounds with an (S)-methyl group on the benzyl linker and different substituents on the bisthiazole core; the results are outlined in **Table 3**. When R_1 and R_2 were alkyl groups, the compounds showed slightly better inhibitory activity than **H6a** (IC_{50} values of 10-20 nM, compounds **H10-12**, **Table 3**). Aromatic substituents such as a phenyl group at the 4' position on the left-hand thiazole ring greatly improved the potency against HDACs, and substituents on this phenyl ring were tolerated (compounds **H14** and **H15**, **Table 3**). The IC_{50} value of compound **H13** was only 4 nM on HDACs (**Table 3**), and it was selected for further evaluation on a cellular level as well as an in vivo efficacy study.

Table 3. Inhibitory activity against human HDACs

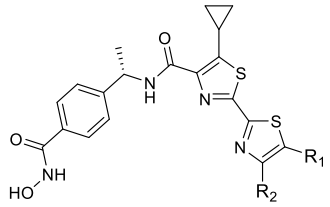

Compound	R_1	R_2	IC_{50}(nM)		
			HDAC1	HDAC3	HDAC6
H6a	H	H	40.92±0.41	42.51±3.04	14.02±1.74
H10	Me	H	19.87±0.47	17.06±0.34	18.51±0.45
H11	H	Me	16.52±0.50	13.88±0.31	19.08±1.55
H12	Cyclohexyl		14.68±0.67	11.35±0.11	18.31±0.84
H13	Ph	H	3.64±0.26	3.02±0.03	4.96±1.86
H14	4-F-Ph	H	2.64±0.02	2.54±0.28	2.02±0.10
H15	4-OMe-Ph	H	3.57±0.40	3.78±0.93	2.38±0.17
LBH589			7.03±1.18	5.83±1.09	10.63±1.30

Compound **H13** was also evaluated in a panel of 11 HDACs and related 3 SIRTs, as listed in **Table 4**. Compound **H13** inhibits HDACs 1, 2, 3, 5, 6, 8, 10, and 11 in nanomole potency and did not inhibit HDACs 4, 7 or 9 or any of the SIRTs.

Table 4. Inhibitory activity of compound **H13** against different HDAC family members and SIRT family members.

Compound		**H13**	LBH589
IC_{50}(nM)	HDAC1	3.59±0.34	7.03±1.18
	HDAC2	13.26±2.04	22.83±0.87
	HDAC3	5.61±1.28	5.83±1.09
	HDAC4	>20000	10390±880
	HDAC5	16740±1520	>20000
	HDAC6	1.59±0.16	6.09±0.73
	HDAC7	>20000	>20000
	HDAC8	16.84±4.23	19.79±4.58
	HDAC9	>20000	>20000
	HDAC10	1.98±0.57	10.24±3.17
	HDAC11	77.82±29.63	121±33
	SIRT1	>20000	>20000
	SIRT2	>20000	>20000
	SIRT3	>20000	>20000

Efficacy of compound **H13** on the cellular level

While compound **H13** was identified as a potent novel inhibitor for HDACs of class I and II, we evaluated its antiproliferative activity in a panel of solid tumor cell lines. LBH589 (panobinostat) was used as the control, and potency was assessed based on the concentration required to inhibit 50% of cell growth at 72 h. As is shown in **Table 5**, Compound **H13** displayed highly potent antiproliferative activities in all the solid tumor cell lines tested (with IC_{50} values less than 200 nM,

Table 5). In particular, compound **H13** showed the most potent antiproliferative activity against NCI-N87 and T47D cells with IC_{50} values of 28 and 40 nM, respectively.

Table 5. Antiproliferation Activity of Compound **H13** Against Several Cancer Cell Lines

Cell line	IC_{50} (nM)	
	H13	LBH589
Human liver cancer cell line BEL-7402	80.79±2.49	21.28±1.61
Human lung adenocarcinoma cell line NCI-H1975	66.38±24.55	17.51±2.23
Human lung squamous cell carcinoma line EBC-1	110±46	27.85±1.72
Human breast cancer cell line MCF-7	58.52±25.72	9.00±0.94
Human breast cancer cell line MDA-MB-231	76.56±31.59	29.13±0.42
Human breast cancer cell line T47D	40.81±16.76	6.98±0.72
Human gastric cancer cell line NCI-N87	28.33±8.67	8.42±0.77
Human colon cancer cell line HT-29	166±7	37.55±4.81

Pharmacokinetic and distribution study of compound **H13**

The pharmacokinetic profiles of compound **H13** are summarized in Table 5. After oral administration of a 5 mg/kg dose of **H13** to mice, **H13** had a C_{max} of 138 ng/mL, $T_{1/2}$ of 4.23 h, and oral bioavailability of 34.4% (**Table 6**).

Table 6. Pharmacokinetic Parameters of Compound **H13**

Compound	Dose	T_{max} (h)	C_{max} (ng/mL)	AUC_{0-t} (ng•h/mL)	$AUC_{0-\infty}$ (ng•h/mL)	MRT (h)	$T_{1/2}$ (h)	F (%)
H13	i.v. 2 mg/kg	/	/	1075	1248	10.4	8.67	
	p.o. 5 mg/kg	0.67	138	924	944	5.22	4.23	34

The metabolic stability of compound **H13** in human, monkey, canine, rat and mouse liver cells was evaluated. Compared to compound **H1**[9], **H13** had better in vivo stability. The mainly metabolism is undergone glucuronic acid binding and amide bond hydrolytic（Information on **H13** metabolites is shown in Table I, SI file). No metabolites related to the phenyl group which attached

to bisthiazole were found, consider the ease of synthesis and the minimum of molecule weight, we chose compound **H13** instead of **H14** or **H15** for the extended profiling and in vivo experiments.

To investigate the distribution of compound **H13** in mice, the concentrations of compound **H13** were determined in tissues and plasma at different time points after oral administration of the mice. Tissue concentrations of compound **H13** were analyzed by LC-MS/MS. The tissue distribution of **H13** in mice showed that the plasma exposure was low in mice after p.o. administration (dose of 50 mg/kg), while high exposure was found in the small intestine and colon. Drug concentrations in tissues after 1 hour were on the following order: stomach> small intestine> liver> kidney> colon> lung> ovary> uterus> plasma> brain> testis. After six hours of administration, **H13** still maintained a high concentration in the colon(**Figure 3A**). The similar results of tissue distribution were found when **H13** was given by intravenous administration. After i.v. administration (dose of 10 mg/kg), high exposure in the small intestine and colon was also found as oral administration (**Figure 3B**).

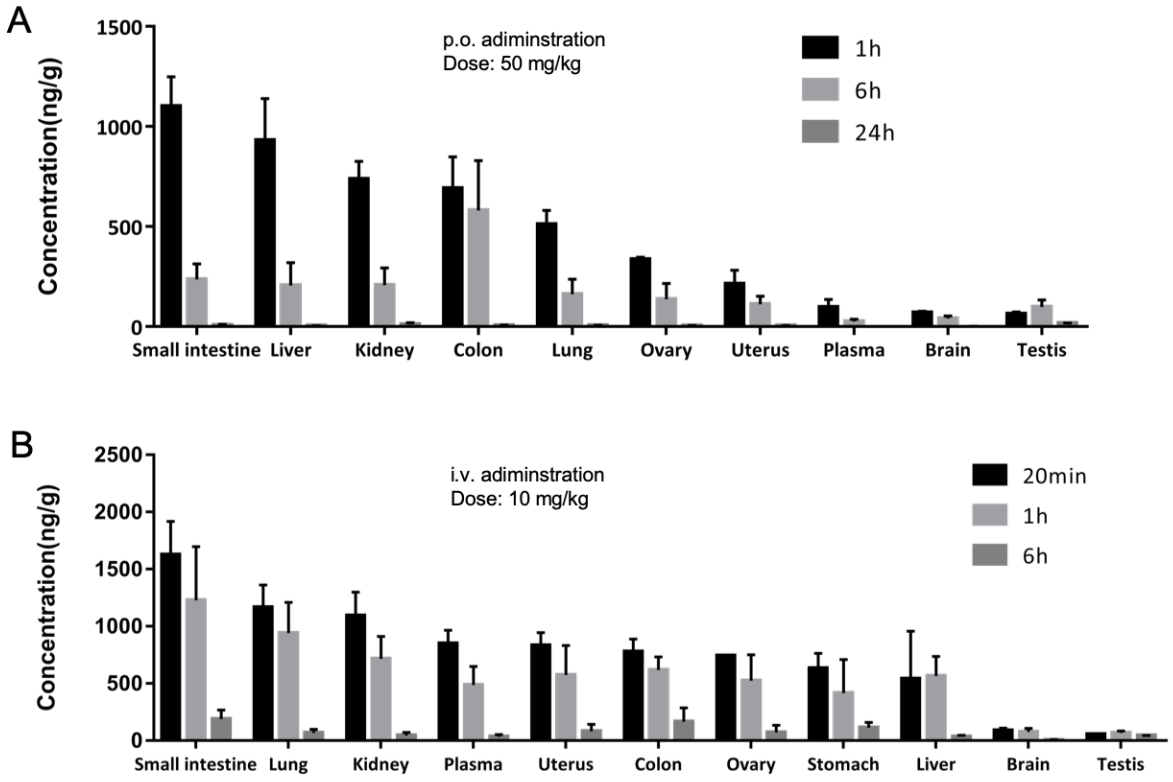

Figure 3. Drug concentration in tissue (A) tissue distribution for oral administration after 1, 6, and 24 hours. (B) tissue distribution for intravenous administration after 0.33, 1, and 6 hours.

AUC is an important parameter for pharmacokinetic analyses, it represents the total drug exposure integrated over time (**Table 7**). The AUC can be applicable to the concentration of drug in tissues. It is the best estimate of drug delivery and an indicator of response. AUCs after the administration of **H13** was in the following order: stomach> colon> small intestine> liver> kidney> lung> ovary> uterus> testis> brain. The compound is distributed in colon in 14.7-fold more in AUC than in plasma. Compound **H13**, as a novel bisthiazole HDAC with an α-(S)-methyl-substituted benzyl

group linker, was therefore identified as a potent and high tissue specificity HDAC inhibitor and moved forward into in vivo studies.

Table 7. The AUC of **H13** in tissues and plasma

Tissue	AUC (ng•h/g)	Rate (Tissue/Plasma)
stomach	105642	176.5
colon	8795	14.7
small intestine	6079	10.2
liver	5185	8.66
kidney	4692	7.84
lung	3438	5.74
ovary	2622	4.38
uterus	1964	3.28
testis	1472	2.46
brain	698	1.17
plasma	599	1

In Vivo Antitumor Efficacy

Because compound **H13** has favorable colon tissue specificity, we chose a human colorectal carcinoma HT-29 xenograftas the solid tumor model for preliminary evaluation and LBH589 as the control. The data are outlined in **Table 8** and **Figure 3**. Compound **H13** demonstrated significant antitumor activity with T/C % = 37.56%, 59.26%, and 60.58% at the oral administration of doses of 100 mg/kg, 50 mg/kg and 25 mg/kg, respectively (Table 8, Figure 3). At the same dose (50 mg/kg), compound **H13** was much more effective than LBH589 (T/C = 59.72% vs 93.85%, **Table 7**). Compound **H13** also showed an acceptable safety profile as indicated by body weight changes.

Table 8 Efficacy of Orally Administered compound **H13** in a HT-29 Xenograft Model

Compound	Dose	n		Weight (g)		TV (mm^3, mean±SD)		RTV (mean±SD)	T/C (%)
		d0	d21	d0	d21	d0	d21		
Vehicle	p.o.	12	12	18.1	19.1	173±38	2854±940	16.68±5.10	
LBH589	50 mg/kg p.o.	6	2	18.2	17.8	173±34	2583±863	15.66±5.97	93.85
H13	100 mg/kg p.o.	6	6	18.7	17.5	169±36	1032±326	6.27±1.98**	37.56
H13	50 mg/kg p.o.	6	6	17.8	18.6	172±44	1602±913	9.96±6.13*	59.72
H13	25 mg/kg p.o.	6	6	17.6	18.5	172±34	1682±398	10.11±3.16*	60.58

t Student's test vs control, *p<0.01

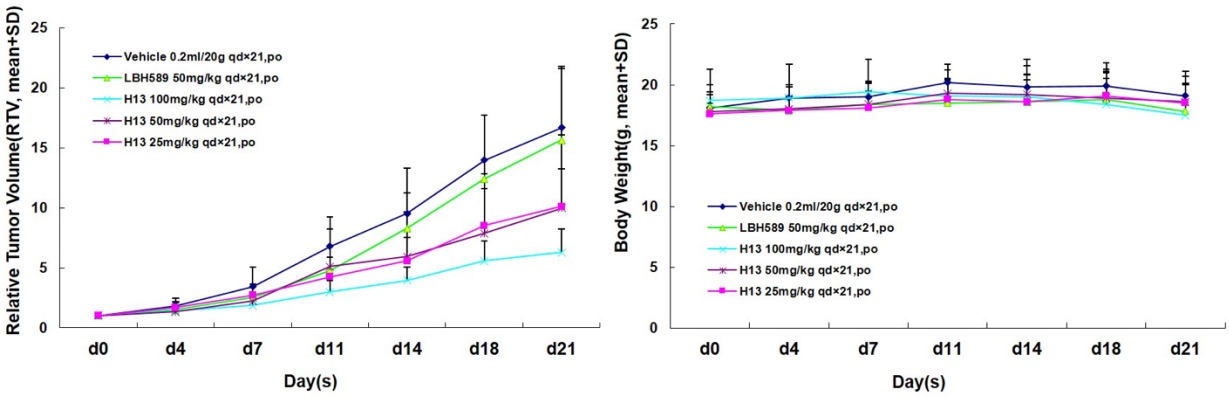

Figure 4. Efficacy of Orally Administered compound **H13** in a HT-29 Xenograft Model

The tumor incidence of compound **H13** in a colitis-associated colorectal cancer model

For evaluation whether compound **H13** directly decreases the incidence of colitis-associated cancer, we generated an AOM-DSS mouse model for colitis-associated colonic tumorigenesis[15] by injecting mice with procarcinogenic AOM followed by 3 cycles of oral DSS administration (**Figure 5A**). The mice were sacrificed on d156 following induction, and the body weight of the mice was monitored throughout the experiment. The tumor incidence was 12.50% and 11.11% in **H13**-treated groups, 100 mg/kg and 50 mg/kg respectively (**Figure 5C** and **Table 9**). The tumor

incidence was 77.78% in the vehicle group as expected, while LBH589 administration showed no effect in this model. Compound **H13** was well tolerated, as the animals showed no signs of toxicity or weight loss over a period of more than 150 days of drug administration (**Figure 5B**).

Table 9. The tumor incidence of compound **H13**

Group	Incidence (%)
Vehicle	77.78
LBH589 50 mg/kg	66.67
H13 100 mg/kg	12.50#
H13 50 mg/kg	11.11#
u test vs vehicle, #p<0.01	

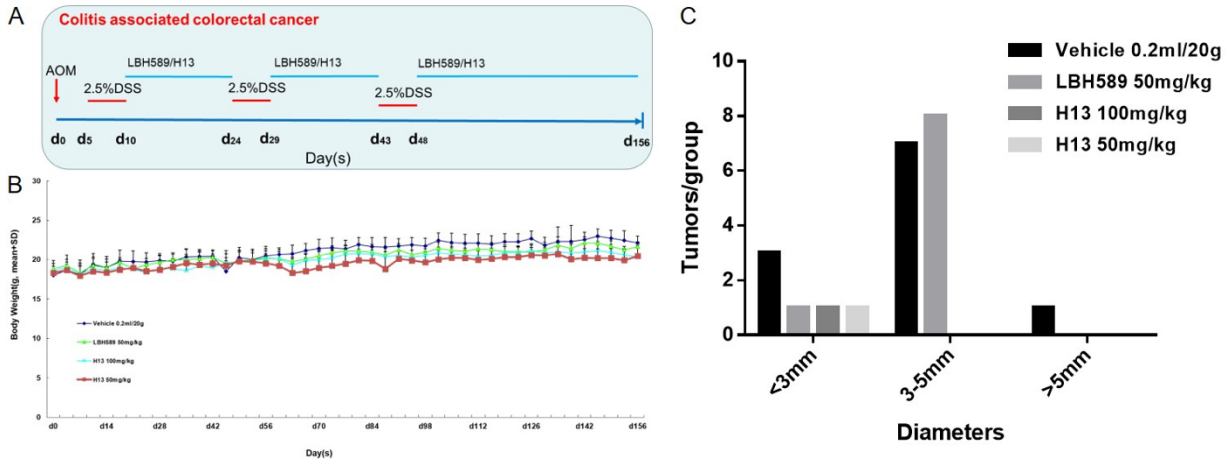

Figure 5. (A) Colitis-associated colorectal cancer model (B) Body weight (C) Tumor diameter and distribution

Although hydroxamic acid has been reported as a mutagen, compounds such as vorinostat and panobinostat based on this structure have demonstrated clinical benefits in hematological malignances. In this study, we also found that after three weeks administration, our compound

exerted potent efficacy against tumor growth in the xenograft models, while nude mice still were in good condition. More importantly, in the model of induced colorectal cancer, we also found that the animals were in good condition after treatment for up to three months. As we know, the AOM-DSS model is an inducible tumorigenesis model. In this model, the compound **H13** did not promote tumorigenesis, but showed promising efficacy. All these data suggest that this compound may have good safety profile. However, other HDAC warheads without mutagenic potential would be a better choice for future modifications.

Conclusion

In conclusion, a series of new bisthiazole HDAC inhibitors was designed and synthesized by replacing the linker group and varying the substituents on the left-hand thiazole ring. Among the prepared compounds, compound **H13**, with an α-(S)-methyl-substituted benzyl group, exhibited excellent inhibitory activity against human HDACs1, 2, 3, 6, 8, 10 with IC_{50} values as low as 4 nM, and it displayed good antiproliferative activity against both hematological malignancy and solid tumor cell lines. Compound **H13** had an acceptable oral bioavailability (F = 34.4%, p.o. 5 mg/kg in mice) and showed high tissue distribution specificity. In efficacy studies, **H13** showed good efficacy in solid tumors such as the HT-29 model. Compound **H13** can also directly decrease the incidence of colitis-associated cancer. All these results indicate that compound **H13** has potential in solid tumor therapy. Further preclinical studies are underway, and the results will be reported in due course.

Experimental Section

General Methods. Starting materials, reagents and solvents were purchased from commercial suppliers and used without further purification. Anhydrous toluene and DCE were obtained from

a distillation over sodium wire or CaH_2. All non-aqueous reactions were run under an inert atmosphere (nitrogen or argon) with rigid exclusion of moisture from reagents and all reaction vessels were oven-dried. Thin-layer chromatography (TLC) was carried out on pre-coated TLC plates with silica gel HSGF 254. Spots were visualized under UV at 254 nm. ^{1}H-NMR and ^{13}C-NMR spectra were measured on a Varian Mercury-VX 300, Varian MR 400, AVANCE III 500 or AVANCE III 600 spectrometer using deuterated chloroform ($CDCl_3$), deuterated methanol (CD_3OD), deuterated acetone (acetone-d_6) and deuterated dimethyl sulfoxide (DMSO-d_6) as the solvent. Chemical shifts are expressed in δ (ppm.). Abbreviations for signal coupling are as follows: s, singlet; brs, broad singlet; d, doublet; t, triplet; q, quartet; dd, double doublet; m, multiplet. Coupling constants (*J*) are given in Hz. HR-MS were measured on a Micromass Ultra Q-Tof. Purity of all final compounds was 95% or higher. Purity was evaluated by analytical HPLC chromatograms using Agilent 1200 series LC system equipped with a degasser, a quaternary pump, an auto sampler, a column oven and a diode array detector. Analytes were separated on a Zorbax SB C18 column (4.6 × 150 mm, 5 μm). Solvent A was 0.1% trifluoroacetic acid in H_2O, and solvent B was 100% methanol. Gradient elution: 20% B for 2 min, then 20%-80% B from 2 to 20 min, 80% B was maintained for 5 min, then 80% -20% B from 25 min to 30 min. All compounds were monitored at 254 nm at room temperature. Flow rate: 1.0 mL/min. The following abbreviations for solvents and reagents are used; N, N-dimethlformamide (DMF), dimethylsulfoxide (DMSO), sodium hydroxide (NaOH), 1,2-dichloroethane (DCE), tetrahydrofuran (THF).

5-Isobutyl-[2,2'-bithiazole]-4-carboxylic acid (1a). Under the protection of N_2, a solution of 2-bromothianzole (5.51g, 0.034mol) was added dropwise to a suspension of activated Zn powder (1.87g, 0.029mol) in dry THF (30mL) and the resulting mixture was heated to reflux for 2h. After the organozinc reagents was obtained, the reaction mixture was cooled to room temperature.

Meanwhile, under the protection of N_2, Pd $(OAc)_2$ (272mg, 1.2mmol), PPh_3 (630mg, 2.4mmol) and methyl 2-bromo-5-isobutylthiazole-4-carboxylate (9.42g, 0.034mol) was add to dry toluene(30mL), and the resulting mixture was stirred under room temperature for 2h. Then the reaction mixture was transfer to the organiczinc reagents, then the obtained mixture was again heated to reflux for several hours until most of methyl 2-bromo-5-isobutylthiazole-4-carboxylate was consumed. The reaction mixture was cooled to room temperature and concentrated under reduced pressure. The residues were diluted with CH_2Cl_2 and the obtained suspension washed with 1N HCl and brine, respectively. The CH_2Cl_2 was dried over anhydrous Na_2SO_4 and concentrated under reduced pressure. The obtained residue was purified by silica gel column chromatography (PE:EtOAc = 20:1-4:1) to afford methyl 5-isobutyl-[2,2'-bithiazole]-4-carboxylate as pale-yellow solids (7.96g, 83%). **^{1}H NMR** (300MHz, $CDCl_3$): δ 7.86 (d, J = 3.3Hz, 1H), 7.46 (d, J = 3.3Hz, 1H), 3.96 (s, 3H), 3.15 (d, J = 6.9Hz, 2H), 1.95-1.23 (m, 1H), 0.99 (d, J = 6.6Hz, 6H); **MS (ESI+)** *m/z*: 283.0 $(M+H)^+$.

To a stirred solution of above obtained coupling product methyl 5-isobutyl-[2,2'-bithiazole]-4-carboxylate (11.28g, 0.04mmol) in MeOH/H_2O (1:4, v/v, 50mL) was added solid NaOH (3.00g, 0.07mmol) at 0℃. The resulting mixture was heated to reflux for 1h and the cooled to room temperature. After removal of MeOH under reduced pressure, the resulting mixture was extracted with Et_2O. The aqueous phase was then acidified with 1N HCl to pH = 2.0, extracted with EtOAc 150mL (50mL×3). The combination EtOAc extract was washed with brine, dried over anhydrous Na_2SO_4 and concentrated under reduced pressure to afford respective acid as a yellow solid **1a**.**^{1}H NMR** (300MHz, $CDCl_3$) δ 7.86 (d, J = 3.3Hz, 1H), 7.46 (d, J = 3.3Hz, 1H), 3.15 (d, J = 6.9Hz, 2H), 1.95-1.23 (m, 1H), 0.99 (d, J = 6.6Hz, 6H); **MS (ESI+)** *m/z*: 269.0$(M+H)^+$.

5-Cyclopropyl-[2,2'-bithiazole]-4-carboxylic acid (1b). 1b was obtained in 75% yield as yellow

solids according to the preparation procedure for **1a.** **^{1}H NMR** (300MHz, $CDCl_3$): δ 7.85 (d, J = 3.0Hz, 1H), 7.45 (d, J = 3.0Hz, 1H), 3.10-3.14 (m, 1H), 1.31-1.38 (m, 2H), 0.84-0.89 (m, 2H); **MS (ESI+)** *m/z*: 267.0$(M+H)^+$.

Methyl 1-(5-isobutyl-[2,2'-bithiazole]-4-carbonyl)piperidine-4-carboxylate (7). To a solution of the bisthiazole carboxyl acid **1a** (70mg, 0.26mmol) in 5mL dry DMF were added EDCI (49mg, 0.26mmol), HOBT (35mg, 0.26mmol), **19** (40mg, 0.28mmol) and i-Pr_2NEt (99mg, 0.75mmol), respectively. The resulting mixture was stirred for 12h at room temperature. Then the mixture was diluted with H_2O and extracted with EtOAc (10mL×3). The combined organic phase was washed with brine, dried over anhydrous Na_2SO_4, and then concentrated under reduced pressure The obtained residue was purified by silica gel column chromatography (PE:EtOAc =10:1) to afford **26** (yellow oil, 81.7%).**^{1}H NMR** (300MHz, CD_3OD) δ 7.89 (d, J = 3.3Hz, 1H), 7.71 (d, J = 3.3Hz, 1H), 4.49 (d, J = 13.2Hz, 1H), 3.82(s, 3H), 3.77 (d, J = 13.8Hz, 1H), 3.07-3.26 (m, 2H), 2.84 (d, J = 7.2Hz, 2H), 2.63-2.70 (m, 1H), 1.87-1.99 (m, 2H), 1.66-1.80 (m, 2H), 0.99 (d, J=6.6Hz, 6H) 3.15 (d, J = 6.9Hz, 2H), 1.95-1.23 (m, 1H).

8-13 was synthesized following procedures similar to that described for compound **7**

Methyl 4-(5-isobutyl-[2,2'-bithiazole]-4-carboxamido)benzoate (8). **^{1}H NMR** (300MHz, $CDCl_3$) : δ 9.47 (s, 1H), 8.03 (d, J = 8.7Hz, 2H), 7.88 (d, J = 3.3Hz, 1H), 7.78 (d, J = 8.4Hz, 2H), 7.48 (d, J = 3.3Hz, 1H), 3.89 (s, 3H), 3.30 (d, J = 7.2Hz, 2H), 2.02-2.07 (m, 1H), 1.02 (d, J = 6.6Hz, 6H). **^{13}C NMR** (75MHz, $CDCl_3$): δ 166.8, 160.6, 160.0, 156.9, 149.8, 144.3, 143.3, 142.1, 131.0, 125.7, 121.6, 119.1, 52.2, 36.1, 31.2, 22.5, 22.4.

Methyl (E)-3-(4-(5-isobutyl-[2,2'-bithiazole]-4-carboxamido)phenyl)acrylate (9) **^{1}H NMR** (300MHz, $CDCl_3$) : δ 9.04 (s,1H), 8.03 (d, J = 8.7Hz, 2H), 7.89 (d, J = 3.3Hz, 2H), 7.47 (d, J = 16Hz, 1H), 6.45 (d, J = 16Hz, 1H), 3.89 (s, 3H), 3.23 (d, J = 7.2Hz, 2H), 2.01-1.98 (m, 1H), 1H), 0.96 (d, J = 6.6Hz, 6H);

Methyl 4-(1-(5-cyclopropyl-[2,2'-bithiazole]-4-carboxamido)ethyl)benzoate (11). **^{1}H NMR** (300MHz, $CDCl_3$) δ 8.03 (d, J = 8.1Hz, 2H), 7.72 (d, J = 3.3Hz,1H), 7.65 (d, J = 8.1Hz, 1H), 7.49

(d, *J* = 8.1Hz, 1H), 7.44 (d, *J* = 3.3Hz,1H), 5.40-5.28 (m, 1H), 3.91 (s, 3H), 3.47–3.38 (m, 1H), 1.65 (d, *J*=7.2Hz, 3H), 1.33-1.28 (m, 2H), 0.82-0.78 (m, 2H); **MS (ESI+)** m/z: 436.1(M+Na)$^+$.

Benzyl 4-(1-(5-cyclopropyl-[2,2'-bithiazole]-4-carboxamido)cyclopropyl)benzoate (12). ^{1}H NMR (300MHz, $CDCl_3$) δ 8.01 (d, *J* = 8.7Hz, 1H), 7.85 (d, *J* = 3.0Hz, 1H), 7.44 (d, *J* = 3.0Hz, 1H), 5.34 (s, 2H), 3.89 (s, 3H), 3.49-3.38 (m, 1H), 1.53-1.42 (m, 4H), 1.35-1.28 (m, 2H), 0.83-0.78 (m, 2H); **MS (ESI+)** *m/z*: 524.1(M+Na)$^+$.

methyl 4-(1-(5-cyclopropyl-[2,2'-bithiazol]-4-yl)-2-methyl-1-oxopropan-2-yl)benzoate (13). ^{1}H NMR (300MHz, $CDCl_3$) δ 8.03 (d, *J* = 8.7Hz, 2H), 7.86 (d, *J* = 3.0Hz,1H), 7.80 (s, 1H), 7.54 (d, *J* = 8.7Hz, 2H), 7.45 (d, *J* = 3.0Hz,1H), 4.36 (q, *J* = 7.2Hz, 2H), 3.41–3.32 (m, 1H), 1.83 (s, 6H), 1.37 (d, *J* = 7.2Hz, 3H), 1.28-1.23 (m, 2H), 0.79-0.74 (m, 2H); **MS (ESI+)** *m/z*: 464.1(M+Na)$^+$.

methyl (S,E)-4-(((tert-butylsulfinyl)imino)methyl)benzoate (16a). To a solution of **14** (5.00g, 30.5mmoL) in 150mL dry DCM were added **15a** (4.43g, 36.6mmoL), $CsCO_3$ (12.9g, 36.6mmoL), the mixture was stirred for 18h at reflux temperature, and then concentrated under reduced pressure, then the mixture was diluted with H_2O and extracted with EtOAc. The resulting mixture use diatomite to filter. The combined organic phase was washed with brine, dried over anhydrous Na_2SO_4, and then concentrated under reduced pressure The obtained residue was purified by silica gel column chromatography (PE:Acetone=4:1) to afford **16a**.^{1}H NMR (300MHz, $CDCl_3$) δ 8.63 (s, 1H), 8.13 (d, *J* = 8.4Hz, 2H), 7.91 (d, *J* = 8.4Hz, 2H), 3.94 (s, 3H), 1.27 (s, 9H); MS (ESI+) m/z: 290.1(M+Na)$^+$.

Methyl (S,E)-4-(2-(tert-butylsulfinyl)vinyl)benzoate (16b). 16b was synthesized following procedures similar to that described for compound **16a.**

Methyl 4-((S)-1-(((S)-tert-butylsulfinyl)amino)ethyl)benzoate (17a). To the solution of Et_2Zn (17mL, 1M in Toluene, 17mmoL) in 50mL dry THF was added MeMgBr (15mL, 1M in Toluene, 15mmoL) at room temperature. After stirred for 30min, the mixture was cooled to -78^{o}C, the **16a** (2.67g, 10 mmoL) in 15mL dry THF was added. The mixture was stirred for 4h at -78^{o}C. After the mixture was heat up to room temperature. Then the mixture was diluted with saturated and ammonium chloride solution and extracted with EtOAc. The combined organic phase was washed with brine, dried over anhydrous Na_2SO_4, and then concentrated under reduced pressure The obtained residue was purified by silica gel column chromatography (PE: Acetone=4:1) to afford **17a. ^{1}H NMR** (300MHz, $CD3Cl_3$) δ 8.01 (d, *J* = 8.4Hz, 2H), 7.42 (d, *J* = 8.4Hz, 2H), 4.59 (dq, *J*

= 6.6Hz, 3.3Hz, 3H), 1.23 (s, 9H); **MS (ESI+)** *m/z*: 306.1(M+Na)$^+$.

*Methyl 4-((S)-1-(((S)-tert-butylsulfinyl)amino)-2-methylpropyl)benzoate (**17b**).* **17b** was synthesized following procedures similar to that described for compound **36a. ^{1}H NMR (**300MHz, $CDCl_3$) δ 8.01 (d, J = 8.4Hz, 2H), 7.41 (d, J = 8.4Hz, 2H), 4.63 (dq, J = 6.3Hz, 3.3Hz, 3H), 1.20 (s, 9H); **MS (ESI+)** *m/z*: 306.1(M+Na)$^+$.

Methyl 4-((R)-1-(((R)-tert-butylsulfinyl)amino)ethyl)benzoate (17c). 36c was synthesized following procedures similar to that described for compound **36a ^{1}H NMR** (300MHz, $CDCl_3$) δ 7.99 (d, J = 6.9Hz, 2H), 7.33 (d, J = 6.9Hz, 2H), 4.19 (t, J = 5.7Hz,1H), 3.90 (s, 3H), 3.47 (d, J = 5.1Hz, 1H), 2.27-2.14 (m, 1H), 1.23 (s, 9H), 0.92 (dd, J = 6.9Hz, 3H), 0.79 (d, J = 6.9Hz, 2H); **MS (ESI+)** *m/z*: 334.2(M+Na)$^+$. $[\alpha]_D^{20}$ =+33.4 (c 1.81, $CHCl_3$). This sample was measured on an Autopol VI, serial number 90079, manufactured by Rudolph Research Analytical,Hackettstown, NJ. The literature reports that R-configuration compound $[\alpha]_D^{20}$ =-33.4 (c 1.81, $CHCl_3$)[12], **36c** was therefore confirmed as S-configuration compound.

Methyl (S)-4-(1-aminoethyl)benzoate (18a). To a stirred solution of **17a** (1.18g, 4.16 mmoL) in 5mL DCM, 10mL 2N HCl/MeOH was added at 0℃, the mixture was stirred for 3h at room temperature and then concentrated under reduced pressure. The obtained residue hen the mixture was diluted with saturated and sodium carbonate solution and extracted with EtOAc. The combined organic phase was washed with brine, dried over anhydrous Na_2SO_4, and then concentrated under reduced pressure to obtain **18a** without further purification (700mg, 94%, yellow oil).

Methyl (S)-4-(1-amino-2-methylpropyl)benzoate(18b). 18b was synthesized following procedures similar to that described for compound **18a.**

Methyl (R)-4-(1-aminoethyl)benzoate(18c). 37c was synthesized following procedures similar to that described for compound **18a.**

Methyl (S)-4-(1-(5-cyclopropyl-[2,2'-bithiazole]-4-carboxamido)ethyl)benzoate(19a). To a solution of the bisthiazole carboxyl acid **1b** (63mg, 0.25mmoL) in 3mL dry DCM were added **18a** (50mg, 0.28mmoL) and DMAP (45mg, 0.38mmoL), respectively. The resulting mixture was stirred for 10min at room temperature. Then the EDCI (71mg, 0.38mmoL) was added to the resulting mixture under N_2 atmosphere at 0℃. The resulting mixture was stirred for overnight at room temperature. The obtained mixture was diluted with 1N HCl and extracted with EtOAc (10mL×3). The combined organic phase was washed with brine, dried over anhydrous Na_2SO_4,

and then concentrated under reduced pressure The obtained residue was purified by silica gel column chromatography (PE:EtOAc=4:1) to afford **19a**.（79mg, 76.5%, white solid）**^{1}H NMR** (300MHz, $CDCl_3$) δ 8.01 (d, J = 8.1Hz, 2H), 7.82 (d, J = 3.0Hz,1H), 7.66 (d, J = 7.8Hz,1H), 7.47 (d, J = 8.1Hz, 2H), 7.41(d, J = 3.0Hz,1H), 5.37-5.27 (m, 1H), 3.88 (s, 3H), 3.46-3.37 (m, 1H), 1.62 (d, J = 7.2Hz, 3H), 1.31-1.26 (m, 2H), 0.81-0.75 (m, 2H); **MS (ESI+)** *m/z*: 436.4$(M+Na)^+$.

19b,c was synthesized following procedures similar to that described for compound **19a.**

Methyl (S)-4-(1-(5-cyclopropyl-[2,2'-bithiazole]-4-carboxamido)-2-methylpropyl)benzoate(19b). ^{1}H NMR (300MHz, $CDCl_3$) δ 8.02(d, J=8.4Hz, 2H), 7.85(d, J=3.3Hz, 1H), 7.66(d, J=7.8Hz, 1H), 7.45(d, J=3.3Hz, 1H), 7.42(d, J=8.4Hz, 2H), 4.95 (t, J=8.4Hz, 2H), 3.90(s, 3H), 3.45-3.36(m, 1H), 2.26-2.15(m, 1H), 1.32-1.25(m, 2H), 1.05(d, J=6.9Hz, 3H), 0.94(d, J=6.9Hz, 2H), 0.82-0.76(m, 2H), 0.74(d, J=6.0Hz, 6H); **MS (ESI)** *m/z*: 464.1$(M+Na^+)$

Methyl (R)-4-(1-(5-cyclopropyl-[2,2'-bithiazole]-4-carboxamido)ethyl)benzoate(19c). ^{1}H NMR (300MHz, $CDCl_3$) δ 8.03(d, J=8.1Hz, 2H), 7.84(d, J=3.3Hz,1H), 7.66(d, J=7.8Hz,1H), 7.49(d, J=8.1Hz, 2H), 7.43(d, J=3.3Hz,1H), 5.38-5.28(m, 1H), 3.90(s, 3H), 3.47-3.38(m, 1H), 1.64(d, J=6.9Hz, 3H), 1.32-1.28(m, 2H), 0.82-0.77(m, 2H); **MS (ESI)** *m/z*: 436.4$(M+Na^+)$

21e-f was synthesized following procedures similar to that described for compound **19a.**

Methyl (S)-4-(1-(5-cyclopropyl-5'-methyl-[2,2'-bithiazole]-4-carboxamido)ethyl)benzoate(21a). ^{1}H NMR(300MHz, $CDCl_3$) δ 8.03(d, J=8.4Hz, 2H), 7.65(d, J=7.8Hz,1H), 7.50(s,1H), 7.48(d, J=8.4Hz, 2H), 5.39-5.25(m, 1H), 3.91(s, 3H), 3.45-3.37(m, 1H), 2.53 (s, 3H), 1.63 (d, J=6.9Hz, 3H), 1.31-1.27(m, 2H), 0.82-0.76(m, 2H); **MS (ESI)** *m/z*: 450.0$(M+Na^+)$

Methyl (S)-4-(1-(5-cyclopropyl-4'-methyl-[2,2'-bithiazole]-4-carboxamido)ethyl)benzoate(21b). ^{1}H NMR (300MHz, $CDCl_3$) δ 8.03 (d, J= 8.4 Hz, 2H), 7.66 (d, J = 7.8 Hz, 1H), 7.49 (d, J = 8.4 Hz, 2H), 6.99 (s, 1H), 5.37–5.28 (m, 1H), 3.90 (s, 3H), 3.47–3.38 (m, 1H), 2.48 (s, 3H), 1.64 (d, J = 7.2 Hz, 3H), 1.31–1.28 (m, 2H), 0.82–0.76 (m, 2H). **MS (ESI)** *m/z*: 450.1$(M+Na^+)$

Methyl (S)-4-(1-(5-cyclopropyl-2-(4,5,6,7-tetrahydrobenzo[d]thiazol-2-yl)thiazole-4-carboxamido)ethyl)benzoate(21c). **^{1}H NMR** (300MHz, $CDCl_3$) δ 8.02 (d, J = 8.1 Hz, 2H), 7.66 (d, J = 7.8 Hz, 1H), 7.48 (d, J = 8.1 Hz, 2H), 5.36–5.27 (m, 1H), 3.90 (s, 3H), 3.45–3.36 (m, 1H), 2.81 (s, 4H), 1.88 (s, 4H), 1.63 (d, J = 6.9 Hz, 3H), 1.32–1.22 (m, 2H), 0.80–0.73 (m, 2H). **MS (ESI)** *m/z*: 468.2 $(M+H^+)$

Methyl (S)-4-(1-(5-cyclopropyl-5'-phenyl-[2,2'-bithiazole]-4-carboxamido)ethyl)benzoate methyl(21d). **^{1}H NMR**(300MHz, $CDCl_3$) δ 8.04 (d, J = 8.1 Hz, 2H), 8.00 (s, 1H), 7.67 (d, J = 7.8 Hz, 1H), 7.62 (dd, J = 8.1, 1.2 Hz, 2H), 7.51 (d, J = 8.1 Hz, 2H), 7.47–7.36 (m, 3H), 5.40–5.28 (m, 1H), 3.91 (s, 3H), 3.49–3.38 (m, 1H), 1.66 (d, J = 7.2 Hz, 3H), 1.34–1.28 (m, 2H), 0.83–0.78 (m, 2H). **MS (ESI)** *m/z*: 490.1($M+H^+$)

(S)-4-(1-(5-Cyclopropyl-5'-(4-fluorophenyl)-[2,2'-bithiazole]-4-carboxamido)ethyl)benzoate(21e). **^{1}H NMR**(300MHz, $CDCl_3$) δ 8.03 (d, J = 8.1 Hz, 2H), 7.73 (s, 1H), 7.68 (d, J = 7.8 Hz, 1H), 7.60–7.56 (m, 2H), 7.50 (d, J = 8.1 Hz, 2H), 7.13 (t, J = 8.4 Hz, 2H), 5.39–5.29 (m, 1H), 3.91 (s, 3H), 3.47–3.38 (m, 1H), 1.65 (d, J = 6.9 Hz, 3H), 1.33–1.28 (m, 2H), 0.82–0.78 (m, 2H). **MS (ESI)** *m/z*: 508.1($M+H^+$)

Methyl (S)-4-(1-(5-cyclopropyl-5'-(4-methoxyphenyl)-[2,2'-bithiazole]-4-carboxamido)ethyl)benzoate (21f). **^{1}H NMR** (300MHz, $CDCl_3$) δ 8.04 (d, J = 8.4 Hz, 2H), 7.89 (s, 1H), 7.68 (d, J = 8.1Hz, 1H), 7.54 (d, J = 9.0 Hz, 2H), 7.50 (d, J = 8.4 Hz, 2H), 6.98–6.92 (d, J = 9.0 Hz, 2H), 5.39–5.29 (m, 1H), 3.91 (s, 3H), 3.85 (s, 3H), 3.47–3.38 (m, 1H), 1.65 (d, J = 6.9 Hz, 3H), 1.34–1.26 (m, 2H), 0.84–0.77 (m, 2H).

N-hydroxy-1-(5-isobutyl-[2,2'-bithiazole]-4-carbonyl)piperidine-4-carboxamide (H2). To a solution of 7(82mg, 0.21mmol) in 6mL DCM and 3mL MeOH add DBU (63mg, 0.42mmol)，then add hydroxylamine (50 wt. % in water) 0.3mL. The resulting mixture was stirred for 12 hours at 30^{o}C. Then the mixture was acidified with 1N HCl to pH = 5.0-6.0, concentrated under reduced pressure. The obtained residue was dissolved in EtOAc. This EtOAc solution was washed with brine, dried over anhydrous Na_2SO_4 and then concentrated under reduced pressure. The obtained residue was purified by silica gel column chromatography (CH_2Cl_2:MeOH=10:1) to afford compound **H2** (pale yellow solid, 69.2%) **^{1}H NMR** (400MHz, DMSO-d_6) δ 10.49 (s, 1H), 8.73 (s, 1H), 7.99 (d, J = 4Hz, 1H), 7.94 (d, J = 4Hz, 1H), 4.50 (d, J = 12Hz, 1H), 3.66 (d, J = 12Hz, 1H), 3.07(t, J = 12Hz, 1H), 2.81-2.74 (m, 3H), 2.34-2.28 (m, 1H), 1.92-1.86 (m, 1H), 1.76-1.69 (m, 1H), 1.64-1.60 (m, 1H), 1.57-1.51 (m, 1H), 0.92 (d, J=8Hz, 6H); **^{13}C NMR** (100MHz, DMSO-d_6) δ 171.2, 162.7, 160.7, 157.9, 147.7, 144.7, 141.5, 123.4, 46.5, 41.4, 35.1, 30.8, 29.3, 28.6, 22.4, 19.9. HRMS (TOF ESI) calcd for $C_{17}H_{22}N_4O_3S_2$ [M+H]: 395.1206, [M+Na]: 417.1026; found:395.1202, 417.1025. HPLC analysis: retention time = 7.564 min; peak area, 99.76%; eluent A, 0.1% TFA in water; eluent B, CH_3OH; isocratic (1:1) over 30min with a flow rate of 1 mL min^{-1}.

H3-15 was synthesized following procedures similar to that described for compound **H2**

N-(4-(hydroxycarbamoyl)phenyl)-5-isobutyl-[2,2'-bithiazole]-4-carboxamide (H3). **^{1}H NMR** (300MHz, CD_3OD+$CDCl_3$): δ 9.45(s, 1H), 7.60(d, *J*=3.3Hz, 1H), 7.49(s, 4H), 7.35(d, *J*=3.3Hz, 1H), 2.99(d, *J*=5.7Hz, 2H), 1.80-1.71(m, 1H), 0.72(d, *J*=9.0Hz, 6H). 6 (m, 1H), 1.76-1.69 (m, 1H), 1.64-1.60 (m, 1H), 1.57-1.51 (m, 1H), 0.92 (d, *J*=8Hz, 6H); **^{13}C NMR** (125MHz, DMSO-d_6) *δ* 163.3, 160.7, 160.2, 157.1, 147.8, 145.0, 144.6, 141.3, 128.4, 128.0, 124.0, 120.2, 35.4, 31.0, 22.5. HRMS (TOF ESI) calcd for $C_{18}H_{18}N_4O_3S_2$ [M+H]: 403.0893, [M+Na]: 425.0713; found: 403.0891, 425.0716. HPLC analysis: retention time = 6.308min; peak area, 97.73%; eluent A, 0.1% TFA in water; eluent B, CH_3OH; isocratic (1:1) over 30min with a flow rate of 1 mL min^{-1}.

(E)-N-(4-(3-(hydroxyamino)-3-oxoprop-1-en-1-yl)phenyl)-5-isobutyl-[2,2'-bithiazole]-4-carboxamide (H4). **^{1}H NMR** (400MHz, DMSO-*d6*) : δ10.74 (s, 1H), 10.30 (s, 1H), 9.04 (s,1H), 8.03 (s,2H), 7.89 (d, *J* = 8Hz, 2H), 7.47 (d, *J* = 16Hz, 1H), 6.45 (d, *J* = 16Hz, 1H), 3.23 (d, *J* = 8Hz, 2H), 2.01-1.98 (m, 1H), 1.76 (d, *J*=12Hz, 1H), 0.96 (d, *J*=4Hz, 6H); **^{13}C NMR** (100MHz, DMSO-d_6) δ 163.5, 160.5, 160.2, 157.1, 147.7, 145.0, 144.6, 139.9, 138.4, 130.8, 128.5, 124.0, 121.0, 118.2, 35.4, 31.0, 22.5, 21.8, 15.0; HRMS (TOF ESI) calcd for $C_{20}H_{20}N_4O_3S_2$ [M+H]: 429.1050, [M+Na]: 451.0869; found: 429.1059, 451.0869. HPLC analysis: retention time = 5.909 min; peak area, 96.28%; eluent A, 0.1% TFA in water; eluent B, CH_3OH; isocratic (1:1) over 30min with a flow rate of 1 mL min^{-1}.

5-Cyclopropyl-N-(4-(hydroxycarbamoyl)benzyl)-[2,2'-bithiazole]-4-carboxamide (H5). **^{1}H NMR** (500MHz, DMSO-d6): δ 11.18 (s, 1H), 9.00 (s, 1H), 8.96-8.93 (m, 1H), 7.98-7.96 (m,2H), 7.54 (d, *J* = 10Hz, 2H), 7.42 (d, *J* = 5Hz, 2H), 4.54 (d, *J* = 10Hz, 2H), 3.37-3.34 (m, 1H), 1.31-1.27 (m, 2H), 0.82-0.79 (m, 2H), **^{13}C NMR** (125MHz, DMSO-d_6) δ 164.6, 162.1, 160.3, 154.7, 153.8, 144.7, 144.5, 143.4, 131.8, 127.7, 127.4, 123.7, 42.5, 14.3, 10.6. HRMS (TOF ESI) calcd for $C_{18}H_{16}N_4O_3S_2$ [M+H]: 401.0737, [M+Na]: 423.0556; found: 401.0739, 423.0558. HPLC analysis: retention time = 7.078 min; peak area, 98.95%; eluent A, 0.1% TFA in water; eluent B, CH_3OH; isocratic (1:1) over 30min with a flow rate of 1 mL min^{-1}.

5-Cyclopropyl-N-(1-(4-(hydroxycarbamoyl)phenyl)ethyl)-[2,2'-bithiazole]-4-carboxamide (H6). **^{1}H NMR** (300MHz, DMSO-*d*6) *δ* 11.15 (s, 1H), 8.99 (s, 1H), 8.60 (d, *J* = 7.5Hz, 2H), 8.00-7.97 (m, 2H), 7.72 (d, *J* = 7.8Hz, 2H), 7.50 (d, *J* = 7.8Hz, 2H), 5.22-5.17 (m, 1H), 3.25-3.21 (m, 1H), 1.54 (d, *J* = 6.9Hz, 3H), 1.27-1.24 (m, 2H), 0.79-0.77 (m, 2H); **MS (ESI+)** m/z: 415.1 $(M+H)^+$.

(S)-5-Cyclopropyl-N-(1-(4-(hydroxycarbamoyl)phenyl)ethyl)-[2,2'-bithiazole]-4-

carboxamide(H6a). **^{1}H NMR**(300MHz, DMSO-*d*6) δ 11.17(s, 1H), 9.01 (s, 1H), 8.63(d, *J*=8.4Hz, 1H), 7.98 (s, *2*H), 7.71(d, *J*=8.4Hz, 2H),7.50(d, *J*=8.4Hz, 2H), 5.24-5.14(m, 1H), 3.27-3.20(m, 1H), 1.55(d, *J*=6.9Hz, 3H), 1.29-1.20(m, 2H), 0.81-0.75(m, 2H); **MS (ESI)** *m/z*: 437.1(M+Na^+)

(S)-5-Cyclopropyl-N-(1-(4-(hydroxycarbamoyl)phenyl)-2-methylpropyl)-[2,2'-bithiazole]-4-carboxamide(H6b). **^{1}H NMR**(300MHz, DMSO-*d*6) δ 11.15(s, 1H), 9.00 (s, 1H), 8.52(d, *J*=8.7Hz, 1H), 7.97(s, *2*H), 7.72(d, *J*=7.8Hz, 2H), 7.51(d, *J*=7.8Hz, 2H), 4.72(t, *J*=9.0Hz, 1H), 3.20-3.14(m, 1H), 2.35-2.21(m, 1H), 1.25-1.22(m, 2H), 1.03-1.01(m,2H), 0.77(d, *J*=6.0Hz, 6H); **^{13}C NMR** (100MHz, DMSO-*d*6) δ 161.5, 160.3, 154.8, 153.0, 151.2, 145.2, 144.6, 143.7, 132.5, 127.6, 125.8, 123.6, 59.5, 32.6, 20.4, 19.9, 14.2, 14.1, 10.4; **MS (ESI)** *m/z*: 465.1(M+Na^+) HPLC analysis: retention time = 4.445 min; peak area, 98.60%; eluent A, 0.1% TFA in water; eluent B, CH_3OH; isocratic (1:1) over 30min with a flow rate of 1 mL min^{-1}.

5-Cyclopropyl-N-(1-(4-(hydroxycarbamoyl)phenyl)cyclopropyl)-[2,2'-bithiazole]-4-carboxamide (H7). **^{1}H NMR** (400MHz, DMSO-d_6) δ 11.13 (s, 1H), 9.07 (s, 1H), 8.96 (s, 1H), 7.97 (s, 1H) , 7.67 (d, *J* = 8.0Hz, 2H), 7.29 (d, *J* = 8.0Hz, 2H), 3.27-3.23 (m, 1H), 1.41-1.38 (m, 4H), 1.33-1.25 (m, 2H), 0.82-0.78 (m, 2H); **^{13}C NMR** (100MHz, DMSO-d_6) δ 162.7, 160.3, 154.6, 153.8, 147.3, 144.9, 144.5, 130.6, 127.2, 125.1, 123.8, 34.8, 19.3, 14.4, 10.5. HRMS (TOF ESI) calcd for $C_{20}H_{18}N_4O_3S_2$ [M+H]: 427.0893, [M+Na]: 449.0713; found: 427.0891, 449.0708. HPLC analysis: retention time = 4.535 min; peak area, 96.49%; eluent A, 0.1% TFA in water; eluent B, CH_3OH; isocratic (1:1) over 30min with a flow rate of 1 mL min^{-1}.

4-(1-(5-Cyclopropyl-[2,2'-bithiazol]-4-yl)-2-methyl-1-oxopropan-2-yl)-N-hydroxybenzamide (H8). **^{1}H NMR** (500MHz, DMSO-*d6*) δ 11.15 (s, 1H), 8.99 (s, 1H), 8.16 (s, 1H), 7.99 (s, 2H), 7.71 (d, *J*=10Hz, 2H), 7.51 (d, *J*=10Hz, 2H), 3.16-3.12 (m, 1H), 1.74 (s, 6H), 1.26-1.23 (m, 2H), 0.79-0.77 (m, 2H); **^{13}C NMR** (125MHz, DMSO-*d*6) δ 164.7, 161.1, 160.2, 154.6, 153.2, 151.0, 145.2, 144.6, 131.2, 127.2, 125.3, 123.6, 55.7, 29.6, 14.3, 10.4; HRMS (TOF ESI) calcd for $C_{20}H_{20}N_4O_3S_2$ [M+H]: 429.1050, [M+Na]: 451.0869; found: 429.3191, 451.0868. HPLC analysis: retention time = 4.090 min; peak area, 98.68%; eluent A, 0.1% TFA in water; eluent B, CH_3OH; isocratic (1:1) over 30min with a flow rate of 1 mL min^{-1}.

(R)-5-Cyclopropyl-N-(1-(4-(hydroxycarbamoyl)phenyl)ethyl)-[2,2'-bithiazole]-4-carboxamide(H9). **^{1}H NMR**(400MHz, DMSO-*d*6) δ 11.15(s, 1H), 8.99 (s, 1H), 8.61(d, *J*=8.0Hz, 1H), 7.97 (s, *2*H), 7.72(d, *J*=8.0Hz, 2H), 7.50(d, *J*=8.1Hz, 2H), 5.24-5.17(m, 1H), 3.33-3.19(m, 1H), 1.55(d, *J*=8.0Hz, 3H), 1.26-1.24(m, 2H), 0.80-0.78(m, 2H); **^{13}C NMR** (100MHz, DMSO-

*d*6) δ 164.6, 161.4, 160.3, 154.7, 153.5, 148.1, 145.0, 144.5, 131.8, 127.4, 126.7, 123.7, 48.4, 22.1, 14.2, 10.5; HRMS (TOF ESI) calcd for $C_{21}H_{22}N_4O_3S_2$ [M+H]: 415.0893, [M+Na]: 437.0713; found: 415.0885, 437.0710. HPLC analysis: retention time = 4.303 min; peak area, 98.78%; eluent A, 0.1% TFA in water; eluent B, CH_3OH; isocratic (1:1) over 30min with a flow rate of 1 mL min^{-1}.

(S)-5-Cyclopropyl-N-(1-(4-(hydroxycarbamoyl)phenyl)ethyl)-5'-methyl-[2,2'-bithiazole]-4-carboxamide(H10). (45mg, 35.4%, pale yellow solid.**^{1}H NMR** (400MHz, DMSO-*d*6) δ 9.56 (s, 1H), 8.45 (d, *J* = 4 Hz 1H), 7.64 (m, 3H), 7.42 (d, *J* = 4 Hz, 2H), 5.17 (m, 1H), 3.22 (m, 1H), 2.52 (s, 3H),1.54 (d, *J* = 4 Hz, 3H), 1.26-1.24 (m, 2H), 0.77–0.76 (m, 2H). **^{13}C NMR** (125MHz, DMSO-*d*6) δ 161.3, 158.4, 155.0, 152.8, 151.2, 145.5, 144.9, 142.5, 137.7, 132.5, 126.5, 125.9, 48.3, 22.2, 14.1, 12.2, 10.4. HRMS (TOF ESI) calcd for $C_{20}H_{20}N_4O_3S_2$ [M+H]: 429.1050, [M+Na]: 451.0869; found: 428.9721, 451.0864. HPLC analysis: retention time = 4.563min; peak area, 99.59%; eluent A, 0.1% TFA in water; eluent B, CH_3OH; isocratic (1:1) over 30min with a flow rate of 1 mL min^{-1}.

(S)-5-Cyclopropyl-N-(1-(4-(hydroxycarbamoyl)phenyl)ethyl)-4'-methyl-[2,2'-bithiazole]-4-carboxamide(H11). ^{1}H NMR (400MHz, DMSO-*d*6) δ 9.56 (s, 1H), 8.50 (d, *J* = 4 Hz, 1H), 7.63(d, *J* = 4 Hz, 2H), 7.52 (s, 1H), 7.42 (d, *J* = 4 Hz, 2H), 5.18 (m, 1H), 3.23 (m, 1H), 2.41 (s, 3H), 1.54 (d, *J* = 4 Hz, 3H), 1.26 – 1.24 (m, 2H), 0.78 – 0.77 (m, 2H). **^{13}C NMR** (125MHz, DMSO-*d*6) δ 161.3, 159.3, 154.8, 154.0, 153.2, 151.2, 145.6, 145.0, 132.4, 126.5, 125.9, 118.0, 48.3, 22.1, 17.1, 14.2, 10.5. HRMS (TOF ESI) calcd for $C_{20}H_{20}N_4O_3S_2$ [M+H]: 429.1050, [M+Na]: 451.0869; found: 429.1051, 451.0869. HPLC analysis: retention time = 4.472 min; peak area, 97.58%; eluent A, 0.1% TFA in water; eluent B, CH_3OH; isocratic (1:1) over 30min with a flow rate of 1 mL min^{-1}.

(S)-5-Cyclopropyl-N-(1-(4-(hydroxycarbamoyl)phenyl)ethyl)-2-(4,5,6,7-tetrahydrobenzo[d]thiazol-2-yl)thiazole-4-carboxamide(H12). ^{1}H NMR (400MHz, DMSO-*d*6) δ 11.16 (s, 1H), 8.99 (s, 1H), 8.52 (d, *J*=8.0Hz, 1H), 7.72 (d, *J*=8.0Hz, 2H), 7.49 (d, *J*=8.0Hz, 2H), 5.20-5.16 (m, 1H), 3.23-3.18 (m, 1H) , 2.85-2.82 (m, 2H), 2.74-2.71 (m, 2H), 1.82 (s, 3H), 1.54 (d, *J*=8.0Hz, 3H), 1.25–1.21 (m, 2H), 0.78–0.74 (m, 2H). **^{13}C NMR** (100MHz, DMSO-*d*6) δ 164.6, 161.4, 156.3, 155.1, 152.9, 152.0, 148.1, 144.8, 132.8, 131.8, 127.4, 126.7, 48.4, 26.6, 23.6, 23.0, 22.7, 22.1, 14.1, 10.4; HRMS (TOF ESI) calcd for $C_{23}H_{24}N_4O_3S_2$ [M+H]: 469.1363, [M+Na]: 491.1182; found: 469.1363, 491.1179. HPLC analysis: retention time = 12.040 min; peak area, 97.37%; eluent A, 0.1% TFA in water; eluent B, CH_3OH; isocratic (1:1) over 30min with a flow rate of 1 mL min^{-1}.

(S)-5-Cyclopropyl-N-(1-(4-(hydroxycarbamoyl)phenyl)ethyl)-5'-phenyl-[2,2'-bithiazole]-4-

carboxamide(H13). ^{1}H NMR (300MHz, DMSO-*d*6) δ 11.16 (s, 1H), 9.00 (s, 1H), 8.62 (d, *J*=8.1Hz, 1H), 8.40 (s, 1H), 7.80–7.72 (m, 4H), 7.52–7.42 (m, 5H), 5.24–5.19 (m, 1H), 3.27–3.20 (m, 1H), 1.56 (d, *J*=7.2Hz, 3H), 1.28–1.23 (m, 2H), 0.81–0.79 (m, 2H). **^{13}C NMR** (125MHz, DMSO-*d*6) δ 164.6, 161.3, 158.8, 154.5, 153.7, 148.1, 145.1, 141.6, 140.7, 131.8, 130.6, 129.9, 129.6, 127.4, 127.1, 126.7, 48.4, 22.1, 14.3, 10.6. HRMS (TOF ESI) calcd for $C_{25}H_{22}N_4O_3S_2$ [M+H]: 491.1206, [M+Na]: 513.1026; found: 491.1202, 513.1029. $[\alpha]_D^{20}$ =+54.7 (c 1.92, $CHCl_3$). This sample was measured on an Autopol VI, serial number 90079, manufactured by Rudolph Research Analytical, Hackettstown. HPLC analysis: retention time = 12.582 min; peak area, 97.65%; eluent A, 0.1% TFA in water; eluent B, CH_3OH; isocratic (1:1) over 30min with a flow rate of 1 mL min^{-1}.

(S)-5-Cyclopropyl-5'-(4-fluorophenyl)-N-(1-(4-(hydroxycarbamoyl)phenyl)ethyl)-[2,2'-bithiazole]-4-carboxamide(H14). ^{1}H NMR (500MHz, DMSO-*d*6) δ 11.17(s, 1H), 9.00(s, 1H), 8.61(d, *J*=10 Hz, 1H), 8.37(s, 1H), 7.84(d, *J*=10 Hz, 2H), 7.75(d, *J*=5Hz, 2H), 7.52 (d, *J*=10Hz, 2H), 7.37-7.34(m, 2H), 5.23–5.20 (m, 1H), 3.27–3.23(m, 1H), 1.57 (d, *J*=10Hz, 3H), 1.30–1.26 (m, 2H), 0.81–0.80 (m, 2H). **^{13}C NMR** (125MHz, DMSO-*d*6) δ 164.6, 161.9, 161.3, 158.8, 154.4, 153.7, 148.1, 145.1, 140.8, 140.5, 131.8, 129.4, 129.3, 127.4, 127.2, 126.7, 117.0, 116.8, 48.4, 22.2, 14.3, 10.5. HRMS (TOF ESI) calcd for $C_{25}H_{21}FN_4O_3S_2$ [M+H]: 509.1112, [M+Na]: 531.0931; found: 509.1108, 531.0930. HPLC analysis: retention time = 5.230 min; peak area, 95.16%; eluent A, 0.1% TFA in water; eluent B, CH_3OH; isocratic (1:1) over 30min with a flow rate of 1 mL min^{-1}.

(S)-5-Cyclopropyl-N-(1-(4-(hydroxycarbamoyl)phenyl)ethyl)-5'-(4-methoxyphenyl)-[2,2'-bithiazole]-4-carboxamide(H15). ^{1}H NMR (500MHz, DMSO-*d*6) δ 11.17(s, 1H), 9.00(s, 1H), 8.59 (d, *J* =10Hz, 1H), 8.26 (s, 1H), 7.75-7.70(m, 4H), 7.52 (d, *J* = 10Hz, 2H), 7.06(d, *J* = 10Hz, 2H), 5.23–5.21(m, 1H), 3.82(s, 3H), 3.27–3.24 (m, 1H), 2.51(d, *J* = 10Hz, 3H), 1.29–1.25 (m, 2H), 0.82–0.79 (m, 2H). **^{13}C NMR** (125MHz, DMSO-*d*6) δ 164.6, 161.3, 160.4, 157.7, 154.6, 153.4, 148.1, 145.0, 141.8, 139.5, 131.8, 128.6, 127.4, 126.7, 123.1, 115.4, 55.8, 48.4, 22.1, 14.3, 10.5; HRMS (TOF ESI) calcd for $C_{26}H_{24}N_4O_3S_2$ [M+H]: 521.1312, [M+Na]: 531.0931; found: 521.1309, 543.1131. HPLC analysis: retention time = 5.129 min; peak area, 95.74%; eluent A, 0.1% TFA in water; eluent B, CH_3OH; isocratic (1:1) over 30min with a flow rate of 1 mL min^{-1}.

ASSOCIATED CONTENT

Supporting Information

The Supporting Information is available free of charge via the Internet at http://pubs.acs.org.

Additional information for the HDAC Inhibition Assay, pharmacokinetic and distribution study of compound **H13** and descriptions of the colitis-associated colorectal cancer model, docking study，as well as NMR spectrums and HPLC spectrums for compounds **H2-15**, experimental procedures and characterization of new chemical entities (PDF)

Molecular string files for all the final target compounds (CSV)

AUTHOR INFORMATION

Corresponding Author

* Email: fjnan@simm.ac.cn(F.N)

* Email: ychen@simm.ac.cn(Y.C)

* Email: jli@simm.ac.cn(J.L)

ACKNOWLEDGMENTS

Funding Sources

This work was supported by grants from The National Natural Science Foundation of China (30725049), the National Science and Technology Major Project (2018ZX09711002-011-006), the "Personalized Medicines——Molecular Signature-based Drug Discovery and Development", Strategic Priority Research Program of the Chinese Academy of Sciences, Grant No. XDA12020106 , and Shanghai Science and Technology Committee (No. 19431906400).

ABBREVIATIONS USED

SAR, structure-activity relationship; HDAC, Histone deacetylase.

REFERENCES

1. Delcuve, G. P.; Khan, D. H.; Davie, J. R., Roles of Histone Deacetylases in Epigenetic Regulation: Emerging Paradigms from Studies with Inhibitors. Clinical epigenetics. 2012, 4 (1), 5.
2. Falkenberg, K. J.; Johnstone, R. W., Histone Deacetylases and their Inhibitors in Cancer, Neurological Diseases and Immune Disorders. Nat. Rev. Drug. Discov. 2014, 13 (9), 673-691.
3. Mann, B. S.; Johnson, J. R.; Cohen, M. H.; Justice, R.; Pazdur, R., FDA approval summary: Vorinostat for Treatment of Advanced Primary Cutaneous T-cell lymphoma. The oncologist. 2007, 12 (10), 1247-1252.
4. Campas-Moya, C., Romidepsin for the Treatment of Cutaneous T-cell Lymphoma. Drugs today. 2009, 45 (11), 787-795.
5. O'Connor, O. A.; Horwitz, S.; Masszi, T.; Van Hoof, A.; Brown, P.; Doorduijn, J.; Hess, G.; Jurczak, W.; Knoblauch, P.; Chawla, S.; Bhat, G.; Choi, M. R.; Walewski, J.; Savage, K.; Foss, F.; Allen, L. F.; Shustov, A., Belinostat in Patients With Relapsed or Refractory Peripheral T-Cell Lymphoma: Results of the Pivotal Phase II BELIEF (CLN-19) Study. J. Clin. Oncol. 2015, 33 (23), 2492-2499.
6. Shi, Y.; Jia, B.; Xu, W.; Li, W.; Liu, T.; Liu, P.; Zhao, W.; Zhang, H.; Sun, X.; Yang, H.; Zhang, X.; Jin, J.; Jin, Z.; Li, Z.; Qiu, L.; Dong, M.; Huang, X.; Luo, Y.; Wang, X.; Wang, X.; Wu, J.; Xu, J.; Yi, P.; Zhou, J.; He, H.; Liu, L.; Shen, J.; Tang, X.; Wang, J.; Yang, J.; Zeng, Q.; Zhang, Z.; Cai, Z.; Chen, X.; Ding, K.; Hou, M.; Huang, H.; Li, X.; Liang, R.; Liu, Q.; Song, Y.; Su, H.; Gao, Y.; Liu, L.; Luo, J.; Su, L.; Sun, Z.; Tan, H.; Wang, H.; Wang, J.; Wang, S.; Zhang, H.; Zhang, X.; Zhou, D.; Bai, O.; Wu, G.; Zhang, L.; Zhang, Y., Chidamide in Relapsed or Refractory Peripheral T cell Lymphoma: a Multicenter Real-world Study in China. J. Haematol. Oncol. 2017, 10 (1), 69/1-69/5.
7. San-Miguel, J. F.; Hungria, V. T. M.; Yoon, S. S.; Beksac, M.; Dimopoulos, M. A.; Elghandour, A.; Jedrzejczak, W. W.; Guenther, A.; Na Nakorn, T.; Siritanaratkul, N.; Schlossman, R. L.; Hou, J.; Moreau, P.; Lonial, S.; Lee, J. H.; Einsele, H.; Salwender, H.; Sopala, M.; Redhu, S.; Paul, S.; Corrado, C.; Richardson, P. G., Panobinostat plus Bortezomib and Dexamethasone: Impact of Dose Intensity and Administration Frequency on Safety in the PANORAMA 1 trial. *Brit. J. Haematol*. **2017**, 179(1), 66-74.
8. Chun, P., Histone Deacetylase Inhibitors in Hematological Malignancies and Solid Tumors. Arch. Pharm. Res. 2015, 38 (6), 933-949.
9. Chen, F.; Chai, H.; Su, M. B.; Zhang, Y. M.; Li, J.; Xie, X.; Nan, F. J., Potent and Orally Efficacious Bisthiazole-based Histone Deacetylase Inhibitors. ACS. Med. Chem. Lett. 2014, 5 (6), 628-633.
10. Gong, C. J.; Gao, A. H.; Zhang, Y. M.; Su, M. B.; Chen, F.; Sheng, L.; Zhou, Y. B.; Li, J. Y.; Li, J.; Nan, F. J.; Design, Synthesis and Biological Evaluation of Bisthiazole-based Trifluoromethyl Ketone Derivatives as Potent HDAC Inhibitors with Improved Cellular Efficacy. Eur. J. Med. Chem. 2016, 112, 81-90.
11. Bertus, B.; Szymoniak, J., A Direct Synthesis of 1-Aryl- and 1-Alkenylcyclopropylamines

from Aryl and Alkenyl Nitriles. J. Org. Chem. 2003, 68 (18), 7133-7136.
12. Koziara, A.; Zwierzak, A., Iminophosphorane-mediated Transformation of Tertiary Alcohols into t-alkylamines and Their N-phosphorylated Derivatives. Tetrahedron. Lett. 1987, 28 (51), 6513-6516.
13. Fernandez-Salas, J. A.; Maestro, C. M.; Rodrı´guez-Fernandez, M. M.; Garcı´a-Ruano, J. L.; Alonso, I., Intermolecular Alkyl Radical Additions to Enantiopure N-tert Butanesulfinyl Aldimines. Org.Lett. 2013, 15 (7), 1658-1661.
14. Almansa, R.; Guijarro, D.; Yus, M., Synthesis of Highly Enantiomerically Enriched Amines by the Diastereoselective Addition of Triorganozincates to N- (tert-butanesulfinyl) imines. Tetrahedron- *Asymmetr*. 2008, *19* (21), 2484-2491.
15. Guo, W.J.; Sun, Y.; Liu, W.; Wu, X.X.; Guo, L.L.; Cai, P.F.; Wu, X.F.; Wu, X.D.; Shen, Y.; Shu, Y.Q.; Gu, Y.H.; Xu, Q., Small Molecule-driven Mitophagy-mediated NLRP3 Inflammasome Inhibition is Responsible for the Prevention of Colitis-associated Cancer. Autophagy. 2014, 10(6), 972-985.

Table of Contents graphic

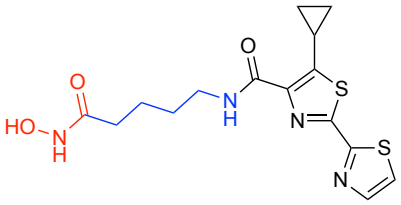

H1(Bisthianostat)

In vitro HDAC1 IC_{50}(uM): 0.081

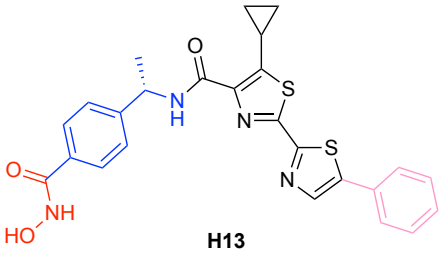

H13

In vitro HDAC1 IC_{50}(uM): 0.004
In vitro cancer cells IC_{50}(uM): 0.011-0.11
F = 34.4%, p.o. 5mg/kg in mice
Ratio(colon/plasma AUC):14.7
Tumor incidence in AOM-DSS Model 11.11% at 50mg/kg. p.o.